ADAPTIVE ROBUST POSTURE CONTROL OF A PNEUMATIC MUSCLES DRIVEN PARALLEL MANIPULATOR [1]

Xiaocong Zhu * **Guoliang Tao** * **Jian Cao** *
Bin Yao *,**

* *The State Key Laboratory of Fluid Power Transmission and Control Zhejiang University, China*
** *School of Mechanical Engineering Purdue University, West Lafayette, IN 47907, USA*

Abstract: Considering rather severe parametric uncertainties and nonlinear uncertainties exist in the dynamic model of pneumatic muscles driven parallel manipulator, a discontinuous projection-based adaptive robust control strategy (ARC) is adopted to effectively handle the effect of various parameter variations of the system and hard-to-model nonlinearities such as the friction forces of the pneumatic muscles and external disturbances of the entire pneumatic system to achieve remarkably precise posture trajectory control. Experimental results are obtained to illustrate the effectiveness of the proposed adaptive robust controller.

Keywords: Pneumatic muscle,Parallel manipulator,Adaptive robust control

1. INTRODUCTION

Pneumatic muscle is a new kind of flexible actuator similar to human muscle, which is made up of rubber tube and cross-weave sheath material. Its basic working principle is as follows: when the rubber tube is inflated, the cross-weave sheath experiences lateral expansion, resulting in axial contractive force and the change of the end point position of pneumatic muscle. Thus, the position or force control of a pneumatic muscle along its axial direction can be realized by regulating the inner pressures of its rubber tube. The parallel manipulator driven by pneumatic muscles (PM by PM) studied in this paper is a new application of pneumatic muscles, which consists of three pneumatic muscles connecting the moving arm of the parallel manipulator to its base platform as shown in Fig.1. By controlling the lengths of three pneumatic muscles, any three-DOF rotation motion of the parallel manipulator can be realized. Such a parallel manipulator combines the advantages of compact structure of parallel mechanisms with the adjustable stiffness and high power/volume ratio of pneumatic muscles, which will have promising wide applications in robotics, industrial automation, and bionic devices.

Severe nonlinearity and time-varying parameters exist in the pneumatic muscle dynamic model; examples include various frictions, hysteresis and the contractive force on the temperature (Lilly, 2003). These factors made the precise position control of a pneumatic muscle alone a significant challenge, which has received great attentions during the past several years. Though significant researches have been done on the control of pneumatic muscles(Lilly, 2003; Bowler *et al.*, 1996;

[1] This work is supported by Festo Inc. through an international cooperation. The last author is supported by the National Natural Science Foundation of China (NSFC) under the Joint Research Fund (grant 50528505) for Overseas Chinese Young Scholars.

Repperger *et al.*, 1998; Tian *et al.*, 2004; Kimoto and Ito, 2003), most of them did not consider the pressure dynamics of the pneumatic muscles, i.e., the dynamics between the inner pressure of the rubber tube and the input flow rate to the pneumatic muscle. The few researches that did consider the pressure dynamics mainly dealt with the controller designs for single or antagonistic muscle actuators, which require accurate system models or disturbance dynamics under matching condition (Hildebrandt *et al.*, 2005).

In this paper, the posture control of a parallel manipulator driven by pneumatic muscles shown in Fig.1 is considered, in which each pneumatic muscle is controlled by two fast switching valves. Such a system not only has all the control difficulties associated with the pneumatic muscles, but also the added difficulty of the coupled multi-input-multi-output (MIMO) complex dynamics of the parallel manipulators. The adaptive robust control strategy(Yao, 2004)is applied to reduce the large extent of lumped unknown uncertain nonlinearities and parametric uncertainties while using certain robust feedback to attenuate the effect of uncompensated model uncertainties. The proposed controller design explicitly takes into account the effect of pressure dynamics as well. Consequently, high tracking performance is achieved in practice as demonstrated by the obtained comparative experimental results.

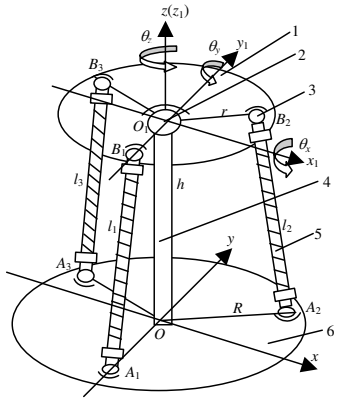

1. Moving platform 2. Ball joint 3. Spherical joint
4. Central pole 5. Pneumatic muscle 6. Base platform

Fig. 1. Structure of the pneumatic muscles driven parallel manipulator

2. DYNAMIC MODELS

The geometric structure of the parallel manipulator is shown in Fig.1, which consists of a moving platform, a base platform, a central pole and three pneumatic muscles. Pneumatic muscles are linked with the moving platform and the base platform by spherical joints, which are evenly distributed along a circle on the respective platform. The central pole is rigidly fixed with the base platform and is connected with the moving platform by a ball joint. The posture of the parallel manipulator is defined through three independent angles: the roll angle θ_x around x, pitch angle θ_y around y, and yaw angle θ_z around z. Two fast switching valves are used to regulate the pressure of each pneumatic muscle, and this combination of components is referred to as a driving unit subsequently.

Let the inertial matrix of the moving platform be $\boldsymbol{I}(\boldsymbol{\theta})$, the transformation matrix from angular velocity to posture vector of the parallel manipulator be $\boldsymbol{G}(\boldsymbol{\theta})$, the coefficient matrix of viscous frictions of the spherical joints be $\boldsymbol{C}_s = diag([c_{s1}, c_{s2}, c_{s3}]^{\mathrm{T}})$, the first-order partial differential kinematic influence coefficient matrix be $\boldsymbol{J}(\boldsymbol{\theta})$, the equivalent mass matrix of three driving units be $\boldsymbol{M}$, the disturbances in task-space be $\boldsymbol{d}_p(t)$ and the muscle force vector be $\boldsymbol{F}_m = [F_{m1}, F_{m2}, F_{m3}]^{\mathrm{T}}$, which will be given in next subsection. Then the dynamic model of the moving platform is (Tao *et al.*, 2005)

$$\boldsymbol{I}_p(\boldsymbol{\theta})\ddot{\boldsymbol{\theta}} + \boldsymbol{B}_p(\boldsymbol{\theta})\dot{\boldsymbol{\theta}} + \boldsymbol{d}_p(t) = \boldsymbol{J}_p^{\mathrm{T}}\boldsymbol{F}_m \qquad (1)$$

where $\boldsymbol{I}_p(\boldsymbol{\theta}) = \boldsymbol{G}^{\mathrm{T}}(\boldsymbol{\theta})[\boldsymbol{I}(\boldsymbol{\theta}) + \boldsymbol{J}^{\mathrm{T}}(\boldsymbol{\theta})\boldsymbol{M}\boldsymbol{J}(\boldsymbol{\theta})]\boldsymbol{G}(\boldsymbol{\theta})$, $\boldsymbol{B}_p(\boldsymbol{\theta}) = \boldsymbol{G}^{\mathrm{T}}(\boldsymbol{\theta})\boldsymbol{C}_s\boldsymbol{G}(\boldsymbol{\theta})$, $\boldsymbol{J}_p(\boldsymbol{\theta}) = \boldsymbol{J}(\boldsymbol{\theta})\boldsymbol{G}(\boldsymbol{\theta})$

For each driving unit i, the muscle force can be described as (Yang *et al.*, 2002; Chou and Hannaford, 1996)

$$F_{mi}(x_{mi}, p_i) = p_i[a(1-k\varepsilon_i)^2 - b] + F_{ri}(x_{mi}) + \delta_{Fi} \qquad (2)$$

where $\varepsilon_i = x_{mi}/L_0$, x_m is the contractive length of the pneumatic muscle, F_r is the compensation for the rubber elastic force, p is the pressure of the pneumatic muscle, a,b are constants related to the structure of pneumatic muscle, k is a factor accounting for the slide effect, and δ_F is the modeling error.

Mass flow rate q_m of air through the valve is a function of the fast switching valve's duty cycle denoted by u

$$q_{mi}(u_i) = u_i A_{ei} \frac{p_{ui}}{RT_{ui}} f\left(\frac{p_{ui}}{p_{di}}\right) \qquad (3)$$

where p_u is the up stream pressure, p_d is the down stream pressure, T_u is the up stream temperature, A_e is the effective orifice area of the valve and R is the gas constant and $f(p_u/p_d)$ is a nonlinear flow function.

A general pressure dynamic equation is(Richer and Hurmuzlu, 2000):

$$\dot{p}_i = \frac{\lambda_{bi} R T_i q_{mi}}{V_i} - \frac{\lambda_{ai} p_i \dot{V}_i}{V_i} \qquad (4)$$

where λ_a and λ_b represent unknown parameters. V is the pneumatic muscle's inner volume and T is the thermodynamic temperature of pneumatic muscle.

From Eq.1, define the drive moment of the parallel manipulator in task-space as $\boldsymbol{\tau}$=$\boldsymbol{J}_p^{\mathrm{T}}(\boldsymbol{\theta})\boldsymbol{F}_m$ and differentiate it to obtain the actuator dynamics.

$$\dot{\boldsymbol{\tau}} = \boldsymbol{f}_\tau(\boldsymbol{\theta},\dot{\boldsymbol{\theta}},\boldsymbol{p}) + \boldsymbol{g}_\tau(\boldsymbol{\theta})\boldsymbol{K}_q(\boldsymbol{p})\boldsymbol{u} + \boldsymbol{d}_\tau(t) \quad (5)$$

where $\boldsymbol{f}_\tau(\boldsymbol{\theta},\dot{\boldsymbol{\theta}},\boldsymbol{p}) = \dot{\boldsymbol{J}}_p^{\mathrm{T}}(\boldsymbol{\theta},\dot{\boldsymbol{\theta}})\bar{\boldsymbol{F}}_m + \boldsymbol{J}_p^{\mathrm{T}}\frac{\partial \bar{\boldsymbol{F}}_m}{\partial \boldsymbol{x}_m}\dot{\boldsymbol{x}}_m - \boldsymbol{J}_p^{\mathrm{T}}\frac{\partial \bar{\boldsymbol{F}}_m}{\partial \boldsymbol{p}}\boldsymbol{A}_f(\boldsymbol{x}_m,\dot{\boldsymbol{x}}_m,\boldsymbol{p})\boldsymbol{\lambda}_a$, $\boldsymbol{g}_\tau(\boldsymbol{\theta})$=$\boldsymbol{J}_p^{\mathrm{T}}\frac{\partial \bar{\boldsymbol{F}}_m}{\partial \boldsymbol{p}}\boldsymbol{A}_g(\boldsymbol{x}_m)\times diag(\boldsymbol{\lambda}_b)$, $\bar{\boldsymbol{F}}_m = \boldsymbol{F}_m - \boldsymbol{\delta}_F$ is the calculable part of $\boldsymbol{F}_m$, $\boldsymbol{d}_\tau(t)$ represents all the unknown disturbances in driving unit space (muscle-space) and $\boldsymbol{K}_q$ is a matrix of nonlinear flow gain function deduced from Eq.3.

Thus, define a set of state variables as $\boldsymbol{x} = [\boldsymbol{x}_1^{\mathrm{T}},\boldsymbol{x}_2^{\mathrm{T}},\boldsymbol{x}_3^{\mathrm{T}}]^{\mathrm{T}} = [\boldsymbol{\theta}^{\mathrm{T}},\dot{\boldsymbol{\theta}}^{\mathrm{T}},\boldsymbol{\tau}^{\mathrm{T}}]^{\mathrm{T}}$, the entire system can be expressed in state-space form as

$$\begin{cases} \dot{\boldsymbol{x}}_1 = \boldsymbol{x}_2 \\ \dot{\boldsymbol{x}}_2 = \boldsymbol{I}_p^{-1}(\boldsymbol{x}_1)[\boldsymbol{x}_3 - \boldsymbol{B}_p(\boldsymbol{x}_1) - \boldsymbol{d}_p(t)] \\ \dot{\boldsymbol{x}}_3 = \boldsymbol{f}_\tau(\boldsymbol{x}_1,\boldsymbol{x}_2,\boldsymbol{p}) + \boldsymbol{g}_\tau(\boldsymbol{x}_1)\boldsymbol{K}_q(\boldsymbol{p})\boldsymbol{u} + \boldsymbol{d}_\tau(t) \end{cases} \quad (6)$$

and $\boldsymbol{p} = \boldsymbol{f}_{\boldsymbol{p}}(\boldsymbol{x}_1,\boldsymbol{x}_3)$ is the inverse function of $\boldsymbol{\tau}$.

3. ADAPTIVE ROBUST CONTROLLER

3.1 Design Issues,Assumptions and Notations

Generally the system is subjected to parametric uncertainties due to the variation of $\boldsymbol{C}_s$, $\boldsymbol{I}_p$, $\boldsymbol{\lambda}_a$, $\boldsymbol{\lambda}_b$ and unknown nonlinearities $\boldsymbol{d}_p$ and $\boldsymbol{d}_\tau$. Practically, $\boldsymbol{d}_p$ and $\boldsymbol{d}_\tau$ may be composed of two parts, a nominal part denoted by $\boldsymbol{d}_{pn}$ and $\boldsymbol{d}_{\tau n}$ which is constant or slowly changing and be dealt with by parameter adaptation, and a fast changing part denoted by $\tilde{\boldsymbol{d}}_p$ and $\tilde{\boldsymbol{d}}_\tau$, which have to be attenuated by the robust feedback.

It can be seen that the major difficulties in controlling are: (a)The system has severe parametric uncertainties represented by the lack of knowledge of the changing damping coefficients $\boldsymbol{C}_s$ and the polytropic exponents $\boldsymbol{\lambda}_a$ and $\boldsymbol{\lambda}_b$. Hence on-line parameter adaptation method should be adopted to reduce parametric uncertainties. (b)The system has a large extent of lumped modeling error like unknown disturbances and unmodeled friction forces, which are contained in $\boldsymbol{d}_p$ and $\boldsymbol{d}_\tau$. So the approach with certain robustness should be used to handle the uncertain nonlinearities for improving effectively performance. (c)The model uncertainties are mismatched, i.e. both parametric uncertainties and uncertain nonlinearities appear in the dynamic equations that are not directly related to the control input $\boldsymbol{u}$. Therefore the backstepping design technology should be employed to overcome design difficulties for achieving asymptotic stability.

Since the extents of parametric uncertainties and uncertain nonlinearities are known, the parametric uncertainties and uncertain nonlinearities are supposed to satisfy $\boldsymbol{\beta} \in \Omega_{\boldsymbol{\beta}} = \{\boldsymbol{\beta} : \boldsymbol{\beta}_{min} \le \boldsymbol{\beta} \le \boldsymbol{\beta}_{max}\}$, and $\tilde{\boldsymbol{d}}_p \le \boldsymbol{d}_{pmax}, \tilde{\boldsymbol{d}}_\tau \le \boldsymbol{d}_{\tau max}$ in which $\boldsymbol{\beta}_{max}$ and $\boldsymbol{\beta}_{min}$ are the maximum and minimum parameter vectors and $\boldsymbol{d}_{pmax}$ and $\boldsymbol{d}_{\tau max}$ are known vectors.

Let $\hat{\boldsymbol{\beta}}$ denote the estimate of $\boldsymbol{\beta}$ and $\tilde{\boldsymbol{\beta}}$=$\hat{\boldsymbol{\beta}}-\boldsymbol{\beta}$ the estimation error. A discontinuous projection can be defined as Eq.7 in order to guarantee that the parameters and their derivatives are bounded in the whole process of adaptive robust control.(Yao *et al.*, 2000)

$$Proj_{\hat{\boldsymbol{\beta}}}(\bullet_i) = \begin{cases} 0, & \text{if } \hat{\boldsymbol{\beta}}_i = \boldsymbol{\beta}_{imax} \text{ and } \bullet_i > 0 \\ 0, & \text{if } \hat{\boldsymbol{\beta}}_i = \boldsymbol{\beta}_{imin} \text{ and } \bullet_i < 0 \\ \bullet_i, & \text{otherwise} \end{cases} \quad (7)$$

The adaptation law is given by

$$\dot{\hat{\boldsymbol{\beta}}} = Proj_{\hat{\boldsymbol{\beta}}}(\boldsymbol{\Gamma}\boldsymbol{\sigma}) \quad (8)$$

where $\boldsymbol{\Gamma} > 0$ is a diagonal matrix and $\boldsymbol{\sigma}$ is an adaptation function to be synthesized later.The projection mapping used in Eq. 8 guaranteed that P1: $\hat{\boldsymbol{\beta}} \in \Omega_{\boldsymbol{\beta}} = \{\boldsymbol{\beta} : \boldsymbol{\beta}_{min} \le \boldsymbol{\beta} \le \boldsymbol{\beta}_{max}\}$ and P2: $\tilde{\boldsymbol{\beta}}^T[\boldsymbol{\Gamma}^{-1}Proj_{\hat{\boldsymbol{\beta}}}(\boldsymbol{\Gamma}\boldsymbol{\sigma}) - \boldsymbol{\sigma}] \le 0$

3.2 ARC Controller Design

The design parallels the recursive backstepping design procedure in task-space and muscle-space via ARC Layapunov functions as follows. (Yao *et al.*, 2000)

1).Step1: Define a switching-function-like quantity as

$$\boldsymbol{z}_2 = \dot{\boldsymbol{z}}_1 + \boldsymbol{K}_c\boldsymbol{z}_1 \quad (9)$$

where $\boldsymbol{z}_1$=$\boldsymbol{x}_1-\boldsymbol{y}_d$ is the trajectory tracking error vector and K_c is a positive diagonal feedback matrix. If $\boldsymbol{z}_2$ converges to a small value or zero, then $\boldsymbol{z}_1$ will converge to a small value or zero since the transfer function from $\boldsymbol{z}_1$ to $\boldsymbol{z}_2$ is stable. Then, differentiating Eq.9 while noting Eq.6,

$$\dot{\boldsymbol{z}}_2 = \boldsymbol{I}_p^{-1}(\boldsymbol{\tau} - \boldsymbol{B}_p\boldsymbol{x}_2 - \boldsymbol{d}_p) - \ddot{\boldsymbol{y}}_d + \boldsymbol{K}_c\dot{\boldsymbol{z}}_1 \quad (10)$$

The unknown parameter vector in task-space is $\boldsymbol{\beta}_p$=$[c_{s1},c_{s2},c_{s3},d_{pn1},d_{pn2},d_{pn3}]^{\mathrm{T}}$ and the term of parametric uncertainties in task-space is described as

$$\hat{\boldsymbol{B}}_p\boldsymbol{x}_2 + \hat{\boldsymbol{d}}_{pn} = -\boldsymbol{\varphi}_2^{\mathrm{T}}\hat{\boldsymbol{\beta}}_p \quad (11)$$

in which $\boldsymbol{\varphi}_2$=$[-diag(\boldsymbol{G}^{\mathrm{T}}\boldsymbol{G}\boldsymbol{x}_2), -\boldsymbol{I}]^{\mathrm{T}}$ is a regressor for parameter adaptation.

If $\boldsymbol{\tau}$ is treated as the input to Eq.10, a virtual control law $\boldsymbol{\tau}_d$ is synthesized such that $\boldsymbol{z}_2$ is as small as possible. $\boldsymbol{\tau}_d$ consists of two terms given by

$$\boldsymbol{\tau}_d = \boldsymbol{\tau}_{da} + \boldsymbol{\tau}_{ds} \quad (12)$$

$$\boldsymbol{\tau}_{da} = \boldsymbol{I}_p(\ddot{\boldsymbol{y}}_d - \boldsymbol{K}_c\dot{\boldsymbol{z}}_1) - \boldsymbol{\varphi}_2^{\mathrm{T}}\hat{\boldsymbol{\beta}}_p \quad (13)$$

in which $\boldsymbol{\tau}_{da}$ functions as the adaptive control law used to achieve an improved model compensation

through on-line parameter adaptation with the adaptation function $\boldsymbol{\sigma}_2 = \boldsymbol{\varphi}_2 \boldsymbol{I}_p^{-\mathrm{T}} \boldsymbol{z}_2$. And $\boldsymbol{\tau}_{ds}$ is a robust control law consisting of two terms for strengthening robust control.

$$\boldsymbol{\tau}_{ds} = \boldsymbol{\tau}_{ds1} + \boldsymbol{\tau}_{ds2}, \quad \boldsymbol{\tau}_{ds1} = -\boldsymbol{I}_p \boldsymbol{K}_2 \boldsymbol{z}_2 \tag{14}$$

where $\boldsymbol{K}_2$ is a positive control gain function,and τ_{ds2} is synthesized to dominate the model uncertainties coming from both parametric uncertainties and uncertain nonlinerities, which is chosen to satisfy the following conditions.

$$\begin{array}{ll} 1. & \boldsymbol{z}_2^{\mathrm{T}}[\boldsymbol{I}_p^{-1}(\boldsymbol{\tau}_{ds2} - \boldsymbol{\varphi}_2^{\mathrm{T}} \tilde{\boldsymbol{\beta}}_p - \tilde{\boldsymbol{d}}_p)] \le \varepsilon_2 \\ 2. & \boldsymbol{z}_2^{\mathrm{T}} \boldsymbol{\tau}_{ds2} \le 0 \end{array} \tag{15}$$

where $\boldsymbol{\varepsilon}_2$ is a positive design parameter.

Let input discrepancy be $\boldsymbol{z}_3 = \boldsymbol{\tau} - \boldsymbol{\tau}_d$, substitute Eq.12 into Eq.10

$$\dot{\boldsymbol{z}}_2 = -\boldsymbol{K}_2 \boldsymbol{z}_2 + \boldsymbol{I}_p^{-1} \boldsymbol{z}_3 + \boldsymbol{I}_p^{-1}(-\boldsymbol{\varphi}_2^{\mathrm{T}} \tilde{\boldsymbol{\beta}}_p - \tilde{\boldsymbol{d}}_p + \boldsymbol{\tau}_{ds2}) \tag{16}$$

For the positive semi-definite(p.s.d) Lyapunov functions V_2 defined by $V_2 = \boldsymbol{z}_2^{\mathrm{T}} \boldsymbol{z}_2/2$, From Eq.16 its time derivative is

$$\dot{V}_2 = -\boldsymbol{z}_2^{\mathrm{T}} \boldsymbol{K}_2 \boldsymbol{z}_2 + \boldsymbol{z}_2^{\mathrm{T}} \boldsymbol{I}_p^{-1} \boldsymbol{z}_3 + \boldsymbol{z}_2^{\mathrm{T}} \boldsymbol{I}_p^{-1}(-\boldsymbol{\varphi}_2^{\mathrm{T}} \tilde{\boldsymbol{\beta}}_p - \tilde{\boldsymbol{d}}_p + \boldsymbol{\tau}_{ds2}) \tag{17}$$

2).Step2: A virtual control input $\boldsymbol{q}_m$ is synthesized so that $\boldsymbol{z}_3$ converges to zero or a small value with a guaranteed transient performance. The derivative of the input discrepancy is

$$\dot{\boldsymbol{z}}_3 = \dot{\boldsymbol{\tau}} - \dot{\boldsymbol{\tau}}_d = \boldsymbol{f}_\tau + \boldsymbol{g}_\tau \boldsymbol{q}_m + \boldsymbol{d}_\tau - \dot{\boldsymbol{\tau}}_{dc} - \dot{\boldsymbol{\tau}}_{du} \tag{18}$$

where $\dot{\boldsymbol{\tau}}_{dc} = \frac{\partial \boldsymbol{\tau}_d}{\partial t} + \frac{\partial \boldsymbol{\tau}_d}{\partial \boldsymbol{x}_1} \hat{\boldsymbol{x}}_2 + \frac{\partial \boldsymbol{\tau}_d}{\partial \boldsymbol{x}_2} \dot{\hat{\boldsymbol{x}}}_2 + \frac{\partial \boldsymbol{\tau}_d}{\partial \hat{\boldsymbol{\beta}}} \dot{\hat{\boldsymbol{\beta}}}$, $\dot{\boldsymbol{\tau}}_{du} = \frac{\partial \boldsymbol{\tau}_d}{\partial t} + \frac{\partial \boldsymbol{\tau}_d}{\partial \boldsymbol{x}_1} \boldsymbol{x}_2 + \frac{\partial \boldsymbol{\tau}_d}{\partial \boldsymbol{x}_2} \dot{\boldsymbol{x}}_2 + \frac{\partial \boldsymbol{\tau}_d}{\partial \hat{\boldsymbol{\beta}}} \dot{\hat{\boldsymbol{\beta}}} - \dot{\boldsymbol{\tau}}_{dc}$, $\hat{\boldsymbol{x}}_2$ and $\dot{\hat{\boldsymbol{x}}}_2$ are deduced from $\boldsymbol{x}_1$ by output differential observer designed in the next part. $\dot{\boldsymbol{\tau}}_{dc}$ is derived from $\boldsymbol{\tau}_d$ and can be used to design control functions, but $\dot{\boldsymbol{\tau}}_{du}$ can not be calculated due to various uncertainties. Let $\tilde{\boldsymbol{d}}_3 = \tilde{\boldsymbol{d}}_\tau - \dot{\boldsymbol{\tau}}_{du}$ be the total uncertainties in muscle-space.

The unknown parameter vector in muscle-space is $\boldsymbol{\beta}_\tau = [\lambda_{a1}, \lambda_{a2}, \lambda_{a3}, \lambda_{b1}, \lambda_{b2}, \lambda_{b3}, d_{\tau n1}, d_{\tau n2}, d_{\tau n3}]^{\mathrm{T}}$, and then the term of parametric uncertainties in muscle-space is described as

$$\hat{\boldsymbol{f}}_\tau + \hat{\boldsymbol{g}}_\tau \boldsymbol{q}_m + \hat{\boldsymbol{d}}_{\tau n} = \boldsymbol{\varphi}_3^{\mathrm{T}} \hat{\boldsymbol{\beta}}_m \tag{19}$$

where $\boldsymbol{\varphi}_3 = [-\boldsymbol{J}_p^{\mathrm{T}} \frac{\partial \bar{\boldsymbol{F}}_m}{\partial \boldsymbol{p}} \boldsymbol{A}_f, \boldsymbol{J}_p^{\mathrm{T}} \frac{\partial \bar{\boldsymbol{F}}_m}{\partial \boldsymbol{p}} \boldsymbol{A}_g diag(\boldsymbol{K}_q \boldsymbol{u}), \boldsymbol{I}]^{\mathrm{T}}$ is a regressor for parameter adaptation. The virtual flow input is given by

$$\boldsymbol{q}_{md} = \boldsymbol{q}_{mda} + \boldsymbol{q}_{mds} \tag{20}$$

$$\boldsymbol{q}_{mda} = \hat{\boldsymbol{g}}_\tau^{-1}(-\boldsymbol{I}_p^{-\mathrm{T}} \boldsymbol{z}_2 - \hat{\boldsymbol{f}}_\tau - \hat{\boldsymbol{d}}_{\tau n} + \dot{\boldsymbol{\tau}}_{dc}) \tag{21}$$

where $\boldsymbol{q}_{mda}$ is used for adaptive model compensation and the adaptation function would be $\boldsymbol{\sigma}_3 = \boldsymbol{\varphi}_3 \boldsymbol{z}_3$. The robust control law $\boldsymbol{q}_{mds}$ consists of the following two terms.

$$\boldsymbol{q}_{mds} = \boldsymbol{q}_{mds1} + \boldsymbol{q}_{mds2}, \quad \boldsymbol{q}_{mds1} = -\hat{\boldsymbol{g}}_\tau^{-1} \boldsymbol{K}_3 \boldsymbol{z}_3 \tag{22}$$

where $\boldsymbol{K}_3$ is a positive feedback gain matrix and $\boldsymbol{q}_{mds2}$ is a robust control function chosen to satisfy the following conditions for dominating all model uncertainties.

$$\begin{array}{ll} 1. & \boldsymbol{z}_3^{\mathrm{T}}[\boldsymbol{q}_{mds2} - \boldsymbol{\varphi}_3^{\mathrm{T}} \tilde{\boldsymbol{\beta}}_\tau + \tilde{\boldsymbol{d}}_3] \le \varepsilon_3 \\ 2. & \boldsymbol{z}_3^{\mathrm{T}} \boldsymbol{q}_{mds2} \le 0 \end{array} \tag{23}$$

where $\boldsymbol{\varepsilon}_3$ is a positive design parameter.

Consider the augmented p.s.d. functions $V_3 = V_2 + \boldsymbol{z}_3^{\mathrm{T}} \boldsymbol{z}_3/2$, its time derivative is

$$\begin{aligned} \dot{V}_3 &= -\boldsymbol{z}_2^{\mathrm{T}} \boldsymbol{K}_2 \boldsymbol{z}_2 + \boldsymbol{z}_2^{\mathrm{T}} \boldsymbol{I}_p^{-1}(-\boldsymbol{\varphi}_2^{\mathrm{T}} \tilde{\boldsymbol{\beta}}_p - \tilde{\boldsymbol{d}}_p + \boldsymbol{\tau}_{ds2}) \\ &\quad -\boldsymbol{z}_3^{\mathrm{T}} \boldsymbol{K}_3 \boldsymbol{z}_3 + \boldsymbol{z}_3^{\mathrm{T}}(-\boldsymbol{\varphi}_3^{\mathrm{T}} \tilde{\boldsymbol{\beta}}_\tau + \tilde{\boldsymbol{d}}_3 + \boldsymbol{q}_{mds2}) \\ &\le -\boldsymbol{z}_2^{\mathrm{T}} \boldsymbol{K}_2 \boldsymbol{z}_2 - \boldsymbol{z}_3^{\mathrm{T}} \boldsymbol{K}_3 \boldsymbol{z}_3 + \boldsymbol{\varepsilon}_1 + \boldsymbol{\varepsilon}_2 \end{aligned} \tag{24}$$

In general, the tracking errors are bounded. Furthermore, in the presence of parametric uncertainties only, asymptotic output tracking or zero final tracking error would be obtained.

3).Step 3: The inverse flow mapping is used to calculate the specific duty cycle command of the fast switching valves for providing the desired flow $\boldsymbol{q}_{md}$. The control input of each valve is

$$\boldsymbol{u} = \boldsymbol{K}_q^{-1} \boldsymbol{q}_{md} \tag{25}$$

3.3 Output Differential Observer

Seen from above, the calculation of Eq.20 need the velocity and acceleration of the posture, therefore an output differential observer (Qi *et al.*, 2003) is proposed for obtaining the velocity and acceleration since it is difficult to establish the observers dependent of the dynamic model due to inaccurate contractive force and friction force of the pneumatic muscle. Let $\hat{x}_{e1i}$, $\hat{x}_{e2i}$, $\hat{x}_{e3i}$ be the estimations of x_{1i}, x_{2i}, $\dot{x}_{2i}$ and $y_i = x_{1i}$ in Eq.26 (the index i represents x, y and z axes respectively).

$$\begin{cases} \dot{\hat{x}}_{e1i} = \hat{x}_{e2i} + a_1(y_i - \hat{x}_{e1i}) \\ \dot{\hat{x}}_{e2i} = \hat{x}_{e3i} + a_2(y_i - \hat{x}_{e1i}) \\ \dot{\hat{x}}_{e3i} = a_3(y_i - \hat{x}_{e1i}) \end{cases} \tag{26}$$

The pole-placement method is utilized to specify the value of a_1, a_2, a_3 according to the expected performance index. The error of output differential observer can be lumped into the uncertain nonlinearity term $\tilde{\boldsymbol{d}}_p$ and $\tilde{\boldsymbol{d}}_\tau$, which can be attenuated by robust control.

3.4 Analysis of Design Parameters

From above procedures, $\boldsymbol{K}_c$, $\boldsymbol{K}_2$, $\boldsymbol{K}_3$, ε_2, ε_3 and adaptation rates $\boldsymbol{\Gamma}_2$, $\boldsymbol{\Gamma}_3$ are the design parameters, which have great effect on system transient performance and final tracking errors.

(a)Large magnitude of $\boldsymbol{K}_c$ contributes to high speed of $\boldsymbol{z}_1$ converging to zero while it is constrained by the bandwidth of the total control

system due to unmodeled dynamics under high frequency, saturation of control variables and limitation of sample frequency etc.

(b)Small magnitudes of ε_2, ε_3 and large magnitudes of $\boldsymbol{K}_2$, $\boldsymbol{K}_3$ are chosen to high control accuracy and transient performance since the solution of Eq.24 is

$$V_3(t) \leq exp(-\lambda_v t)V_3(0)+\frac{\varepsilon_v}{\lambda_v}[1-exp(-\lambda_v t)] \quad (27)$$

where $\lambda_v=2min\{\sigma_{min}(\boldsymbol{K}_2), \sigma_{min}(\boldsymbol{K}_3)\}$, $\sigma_{min}(\cdot)$ denotes the minimum eigenvalue of a matrix and $\varepsilon_v=\varepsilon_2+\varepsilon_3$.

(c)The adaptation rates $\boldsymbol{\Gamma}_2$, $\boldsymbol{\Gamma}_3$ function as adding an integrator of $\boldsymbol{z}_2$ and $\boldsymbol{z}_3$ since the following quasi-stationary equations are deduced by substituting Eq.8 into Eq.16 and Eq.18 respectively.

$$\begin{cases} \dot{\boldsymbol{z}}_2+\boldsymbol{K}_2\boldsymbol{z}_2+\boldsymbol{I}_p^{-1}\boldsymbol{\varphi}_2^{\mathrm{T}}\boldsymbol{\Gamma}_2\int\boldsymbol{\varphi}_2\boldsymbol{I}_p^{-\mathrm{T}}\boldsymbol{z}_2dt+\boldsymbol{I}_p^{-1}\boldsymbol{z}_3=\triangle_2 \\ \dot{\boldsymbol{z}}_3+\boldsymbol{K}_3\boldsymbol{z}_3+\boldsymbol{\varphi}_3^{\mathrm{T}}\boldsymbol{\Gamma}_3\int\boldsymbol{\varphi}_3\boldsymbol{z}_3dt=\triangle_3 \end{cases} \quad (28)$$

where $\triangle_2=-\boldsymbol{I}_p^{-1}\tilde{\boldsymbol{d}}_p$ and $\triangle_3=\tilde{\boldsymbol{d}}_3$ are bounded uncertainties. Then the pole-placement scheme is utilized to design the control gains $\boldsymbol{K}_2$, $\boldsymbol{K}_3$ and $\boldsymbol{\Gamma}_2$, $\boldsymbol{\Gamma}_3$ according to the bandwidth of parallel manipulator and actuator dynamics. However, They are also constrained by the bandwidth of the system as $\boldsymbol{K}_c$.

4. EXPERIMENTAL RESULTS

The effectivenes of the control concept is proved in several measurement plots with the supply pressure being 0.48 MPa. Fig.2 is the experiment set up(Tao *et al.*, 2005). ARC and DRC controllers are tested for comparison in experiments and the performance indexes are as (Yao, 2004).

Fig. 2. Experimental setup of PM by PM

The controllers are first tested for a slow smooth step response with a rise time of 5s shown in Fig.3, in which the response is from posture $\theta_x=0^{\mathrm{o}}$, $\theta_y=0^{\mathrm{o}}$ to posture $\theta_x=6^{\mathrm{o}}$, $\theta_y=-4^{\mathrm{o}}$ (in this system θ_z is ignored since its value is always close to zero). As seen from Fig.3, ARC performs much better than DRC, the final error of ARC is $e_{xF}=0.0195^{\mathrm{o}}$ and $e_{yF}=0.0232^{\mathrm{o}}$ and the max absolute error is $e_{xM}=0.2694^{\mathrm{o}}$ and $e_{yM}=0.4685^{\mathrm{o}}$.

To test the performance robustness of the proposed control to sudden disturbances, the position transducer suffer from a sudden dither, which can be regarded as a sudden large disturbance to the system. The response of this situation is shown in Fig.4. As seen, the system produces large tracking errors due to the wrong feedback information of position transducer, but then after the dither disappeared, the system comes back to the stable posture quickly. Thus, the control algorithm is robust to disturbances.

The controllers are again run for parallel manipulator's tracking sinusoidal motion trajectory with different frequencies. For example, Fig.5 is a sinusoidal motion trajectory with the period of 20s and Fig.6 is the estimated uncertainties in task-space. It is confirmed once more that the ARC achieves much better performances than DRC. The average error of ARC is $L_2[e_x]$=0.1299$^{\mathrm{o}}$ and $L_2[e_y]=0.1012^{\mathrm{o}}$ and the max absolute error is e_{xM}=0.3688$^{\mathrm{o}}$ and e_{yM}=0.3033$^{\mathrm{o}}$. Not surprisingly, the DRC cannot solve the problems of parametric uncertainties or large unmodeled uncertainties, so there are large modeling errors and eventually large tracking errors.

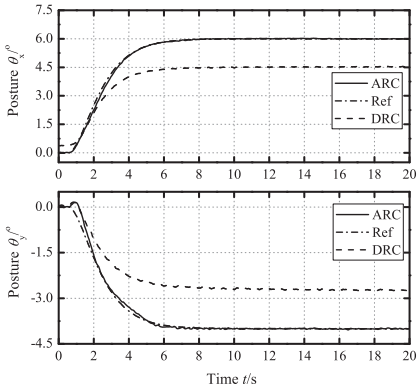

Fig. 3. Smooth step response

5. CONCLUSIONS

The motion trajectory tracking control of a pneumatic muscles driven parallel manipulator controlled by six fast switching valves is considered in the paper. The mathematical models of such a system are subjected to severe parametric uncertainties and uncertain nonlinearities. An adaptive robust controller has been proposed to deal with those model uncertainties effectively. The proposed controller achieves a guaranteed transient performance as well as a guaranteed final tracking accuracy. An output differential observer

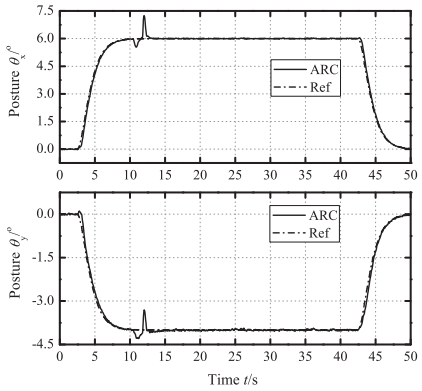

Fig. 4. Performance robustness to sudden disturbance

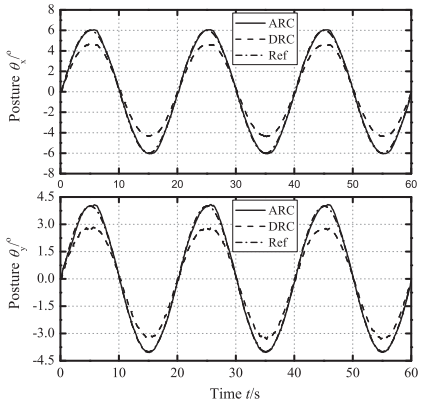

Fig. 5. Sinusoidal motion trajectory

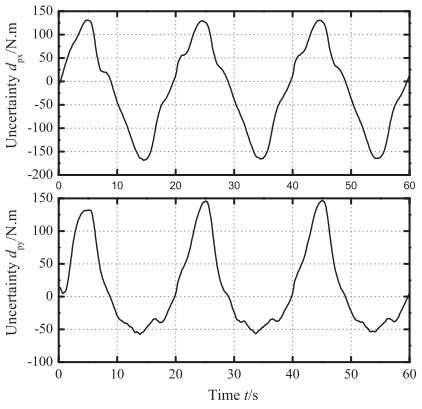

Fig. 6. Estimated uncertainties in task-space

is also constructed to obtain the velocity and acceleration of the parallel manipulator to provide a simple and effective way of implementing the proposed adaptive robust controller. Experimental results have been obtained to verify the good tracking performance of the proposed ARC controller.

REFERENCES

Bowler, C.J., D.G. Caldwell and G.A. Medrano-Cerda (1996). Pneumatic muscle actuators: Musculature for an anthropomorphic robot arm. *IEEE Colloquium on Actuator Technology: Current Practice and New Developments* pp. 8/1–8/6.

Chou, C.P. and B. Hannaford (1996). Measurement and modeling of mckibben pneumatic artificial muscles. *IEEE Transactions on Robotics and Automation* **12**, 90–102.

Hildebrandt, A., O. Sawodny, R. Neumann and A. Hartmann (2005). Cascaded control concept of a robot with two degrees of freedom driven by four artificial pneumatic muscle actuators. In: *American Control Conference*. USA. pp. 680–685.

Kimoto, M. and H. Ito (2003). Nonlinear robust compensation for control of a pneumatic actuator. In: *SICE Annual Conference in Fukui*. Japan. pp. 1820–1825.

Lilly, J.H. (2003). Adaptive tracking for pneumatic muscle actuators in bicep and tricep configurations. *IEEE Transactions on Neural systems and rehabilitation engineering* **11**, 333–339.

Qi, G.Y., Z.Q. Chen and Z.Z. Yuan (2003). High order differential feedback control for nonlinear systems. *Engineering Science* **5**, 35–44.

Repperger, D.W., K.R. Johnson and C.A. Phillips (1998). A vsc position tracking systems involving a large scale pneumatic muscle actuator. In: *Proceedings of the 37th IEEE Conference on Decision and Control*. Tampa,Florida USA. pp. 4032–4037.

Richer, E. and Y. Hurmuzlu (2000). A high performance pneumatic force actuator system: Part i-nonlinear mathematical model. *Transactions of the ASME Journal of Dynamic Systems, Measurement, and Control* **122**, 416–425.

Tao, G.L., X.C. Zhu and J. Cao (2005). Modeling and controlling of parallel manipulator joint driven by pneumatic muscles. *Chinese Journal of Mechanical Engineering(English Edition)* **18**, 537–541.

Tian, S.P., G.Q. Ding, D.T. Yang and L.M. Lin (2004). Nonlinear modeling and controlling of artificial muscle system using neural networks. *Chinese Journal of Mechanical Engineering(English Edition)* **17**, 306–310.

Yang, G., B.R. Li and J. Liu (2002). A new analytical method on characteristics of artificial pneumatic muscle actuator. *Chinese Hydraulics and Pneumatics* **10**, 22–25.

Yao, B. (2004). Advanced motion control: An adaptive robust framework. In: *The 8th IEEE International Workshop on Advanced Motion Control*. Kawasaki Japan. pp. 565–570.

Yao, B., F.P. Bu, J. Reedy and G.T.C. Chiu (2000). Adaptive robust motion control of single-rod hydraulic actuators: Theory and experiments. *IEEE/ASME Transactions on mechatronics* **5**, 79–91.